

## **An improvement of signal-to- noise ratio for phase image**

**Poster No.:** C-0803  
**Congress:** ECR 2017  
**Type:** Scientific Exhibit  
**Authors:** N. Ikemitsu<sup>1</sup>, Y. Kanazawa<sup>1</sup>, Y. Matsumoto<sup>1</sup>, H. Hayashi<sup>2</sup>, T. Usuda<sup>1</sup>, T. Sasaki<sup>1</sup>, M. Miyoshi<sup>3</sup>, M. Harada<sup>1</sup>; <sup>1</sup>Tokushima/JP, <sup>2</sup>Tokushima, Tokushima/JP, <sup>3</sup>Hino/JP  
**Keywords:** MR physics, Computer applications, Contrast agents, MR, Experimental investigations, Computer Applications-General, Physics, Biological effects  
**DOI:** 10.1594/ecr2017/C-0803

Any information contained in this pdf file is automatically generated from digital material submitted to EPOS by third parties in the form of scientific presentations. References to any names, marks, products, or services of third parties or hypertext links to third-party sites or information are provided solely as a convenience to you and do not in any way constitute or imply ECR's endorsement, sponsorship or recommendation of the third party, information, product or service. ECR is not responsible for the content of these pages and does not make any representations regarding the content or accuracy of material in this file.

As per copyright regulations, any unauthorised use of the material or parts thereof as well as commercial reproduction or multiple distribution by any traditional or electronically based reproduction/publication method ist strictly prohibited.

You agree to defend, indemnify, and hold ECR harmless from and against any and all claims, damages, costs, and expenses, including attorneys' fees, arising from or related to your use of these pages.

Please note: Links to movies, ppt slideshows and any other multimedia files are not available in the pdf version of presentations.

[www.myESR.org](http://www.myESR.org)

## Aims and objectives

Transverse relaxation time ( $T_2$ ) is a time constant which includes only nuclear-nuclear interactions.  $T_2^*$  is a time constant including nuclear-nuclear interactions and static magnetic field ( $B_0$ ) inhomogeneity, which is affected by susceptibility. Setting of  $T_2$  or  $T_2^*$  is generally applied to long echo time (TE). It is generally known that the  $T_2^*$  decay is a faster process than the  $T_2$  decay. If a material has strong susceptibility, e.g., blood, FeO, and MR contrast media, the  $T_2^*$  decay is faster.

In magnetic resonance (MR) imaging, a magnitude image takes an absolute value from real and imaginary parts and is used normally in clinical. A phase image made from phase differences of real and imaginary parts which are a reflection of variable information of a local magnetic field. A phase image has good contrast and reveals detail structures that are not visible on the corresponding magnitude image, e.g., it obtains information concerning iron deposit as phase in blood vessels and tissue [1, 2]. The phase image has contrast depending on the susceptibility and TE of each tissue. Moreover, it is used to make a susceptibility weighted image (SWI) [3]. Accordingly, signal-to-noise ratio (SNR) of a phase image is an important factor.

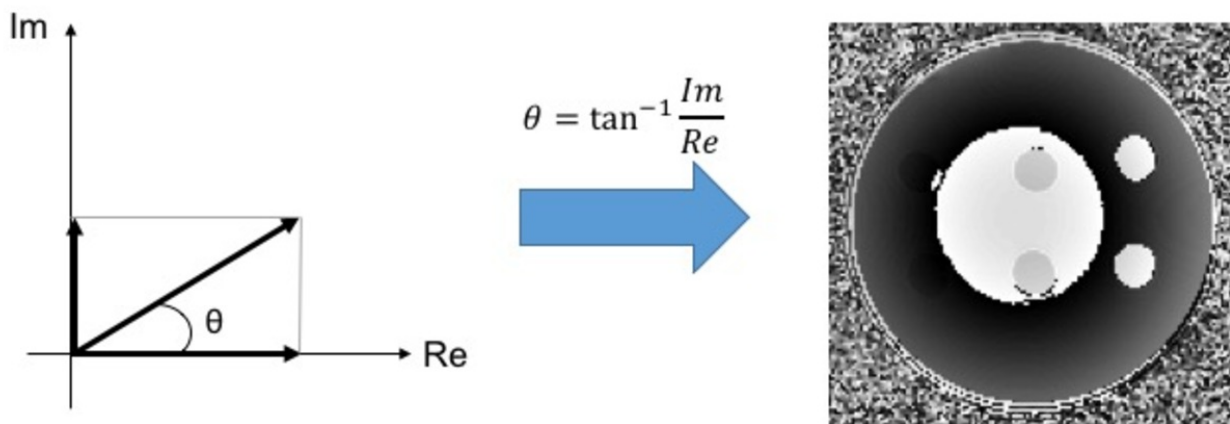


**Fig. 1:** How to make a phase image

**References:** Tokushima University - Tokushima/JP

Wu B et al., have been reported that the SNR of image phase depends on TE, each material's  $T_2^*$ , and offset frequency [4]. Here, we are concerned with the indication of maximum SNR of the image phase when TE is equal to  $T_2^*$ . Therefore, the purpose of this study is to investigate temporal characteristics of the phase SNR, and make a phase image with high SNR by using phase data at the optimized TE. Accordingly, we improve the SNR of the phase image by focusing  $T_2^*$ .

Images for this section:

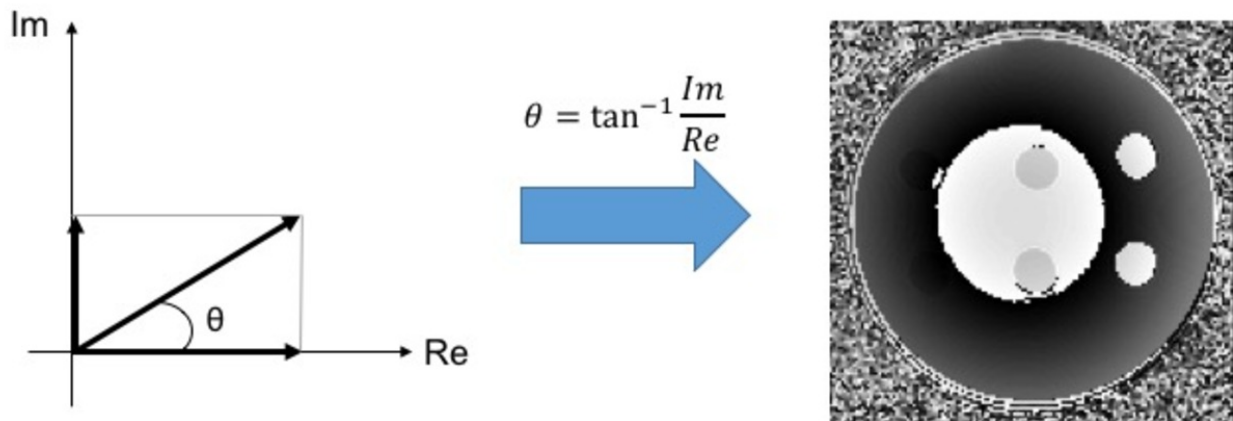


**Fig. 1:** How to make a phase image

© Tokushima University - Tokushima/JP

## Methods and materials

### 1. Phase SNR

In general, theoretical formula of  $T_2^*$  decay is described as follows,

$$M = M_0 e^{-\frac{t}{T_2^*}} \quad (1)$$

#### Fig. 2

**References:** Tokushima University - Tokushima/JP

where is the MR signal, is the transverse magnetization, and is the TE. When the noise variance of real and imaginary channel are equal, noise power in the phase is described by the following equation,

$$\sigma_{\theta}^2 = \left( \frac{1}{M_0 e^{-\frac{t}{T_2^*}}} \sigma \right)^2 \quad (2)$$

#### Fig. 3

**References:** Tokushima University - Tokushima/JP

where represent the noise variance in real or imaginary parts with the noise power. Then, the phase SNR ( $\text{SNR}_{\#}$ ) at is shown as [4],

$$SNR_{\theta} = \frac{2\pi f t}{\sigma_{\theta}} = \frac{2\pi f t M_0 e^{-\frac{t}{T_2^*}}}{\sigma} \quad (3)$$

**Fig. 4**

**References:** Tokushima University - Tokushima/JP

where is the frequency offset. The above equation is differentiated by,

$$\frac{dSNR_{\theta}}{dt} = 0 \Rightarrow t = T_2^* \quad (4)$$

**Fig. 5**

**References:** Tokushima University - Tokushima/JP

the phase becomes maximum when the TE is equal to the  $T_2^*$ . In other words, the  $T_2^*$  is the optimal TE when considering the best .

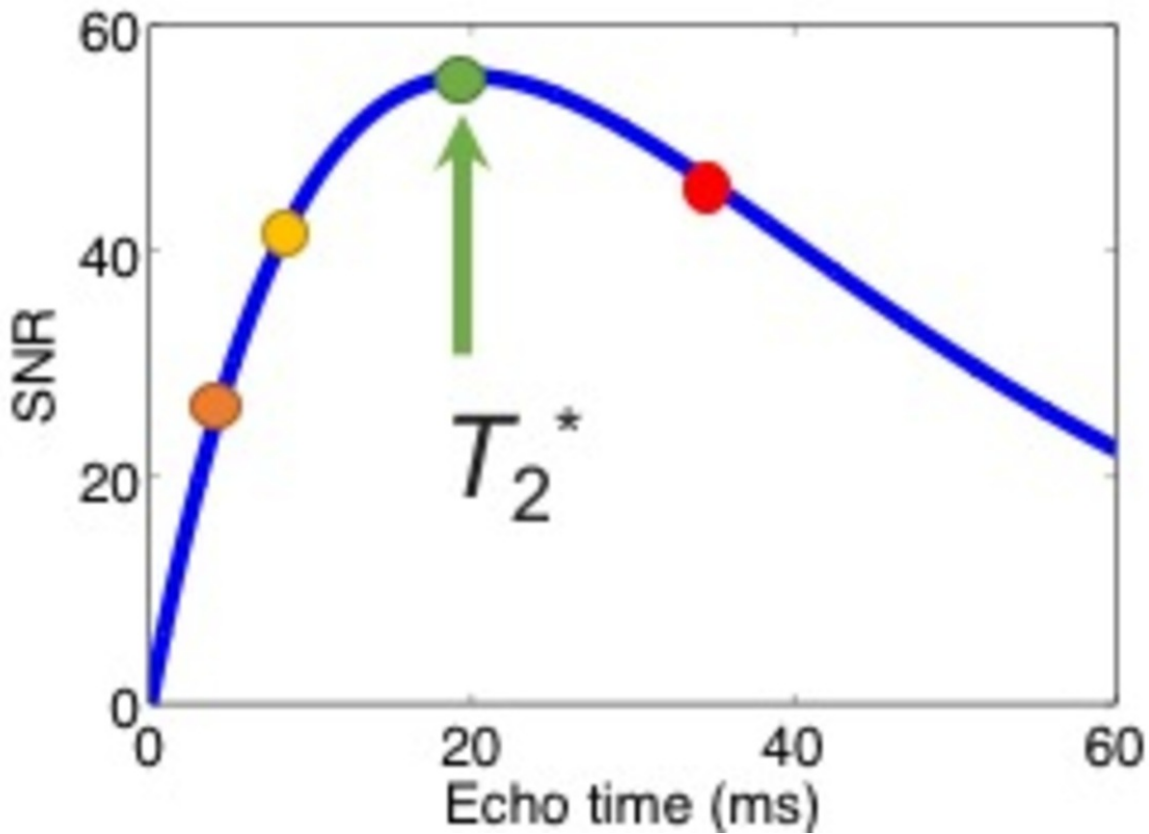


**Fig. 6:** Relationship between TE and phase SNR  
**References:** Tokushima University - Tokushima/JP

## 2. MR imaging

On a 3.0T MRI system, both phantom was acquired with three-dimensional fast spoiled gradient-echo (3D-SPGR). The other imaging parameters are shown in Fig7.

Parameters	Values
TE	16 echoes, from 4.5 to 109 ms ( $\Delta TE = 7$ ms)
TR	114 ms
Flip angle (FA)	30 degrees
Pixel bandwidth (BW)	150 Hz/pixel
Fields of view (FOV)	$192 \times 192 \times 24$ mm <sup>3</sup>
Voxel size	$0.75 \times 0.75 \times 2$ mm <sup>3</sup>

**Fig. 7:** Image parameter  
**References:** Tokushima University - Tokushima/JP

We made a phantom using six tubes of gadopentetate dimeglumine (Gd-DTPA; Magnevist, Bayer Pharma AG, Germany) at different concentrations (0.1, 0.5, and 1.0 wt %) and Gd-DTPA (0.1, 0.5, 1.0 wt%) and with agar (1.0 wt%). The six tubes were fixed in agar (1.0 wt%) and placed within a cylindrical container.

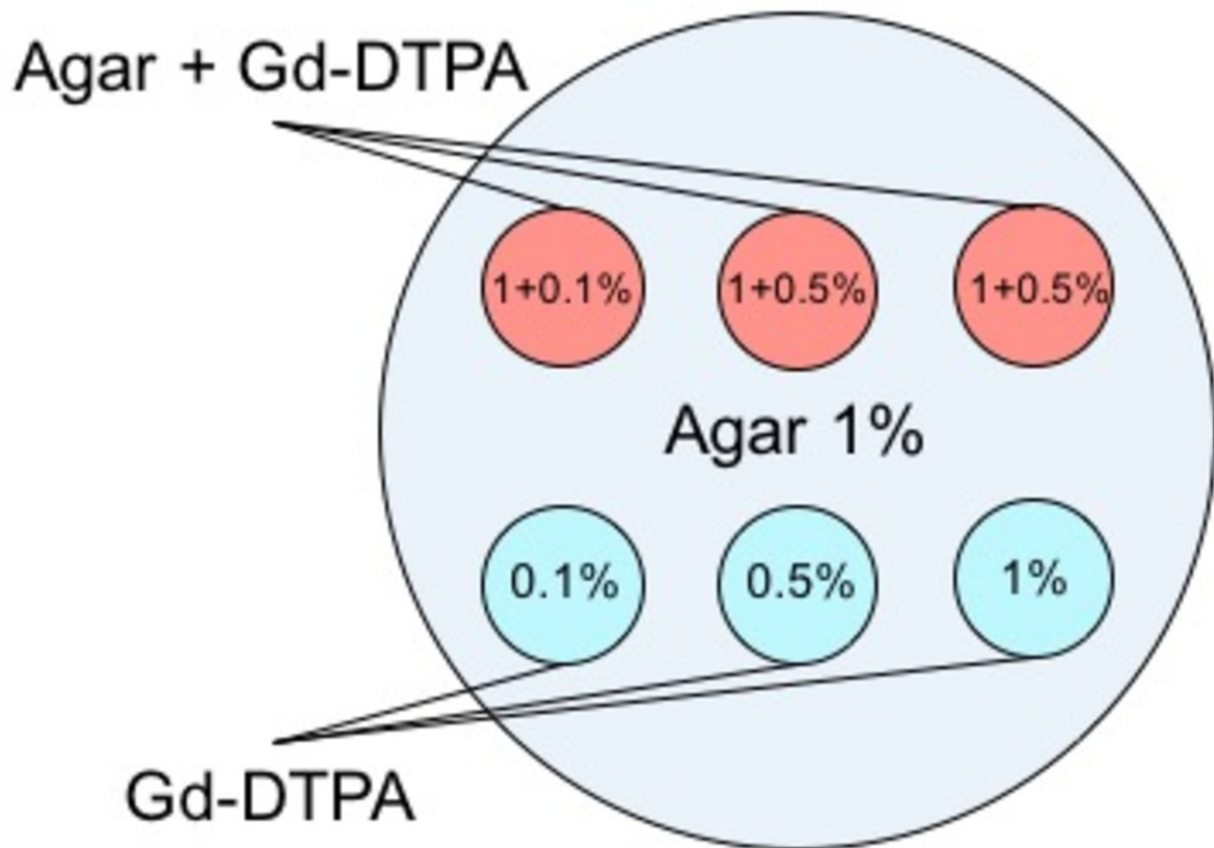


**Fig. 8:** Phantom component

**References:** Tokushima University - Tokushima/JP

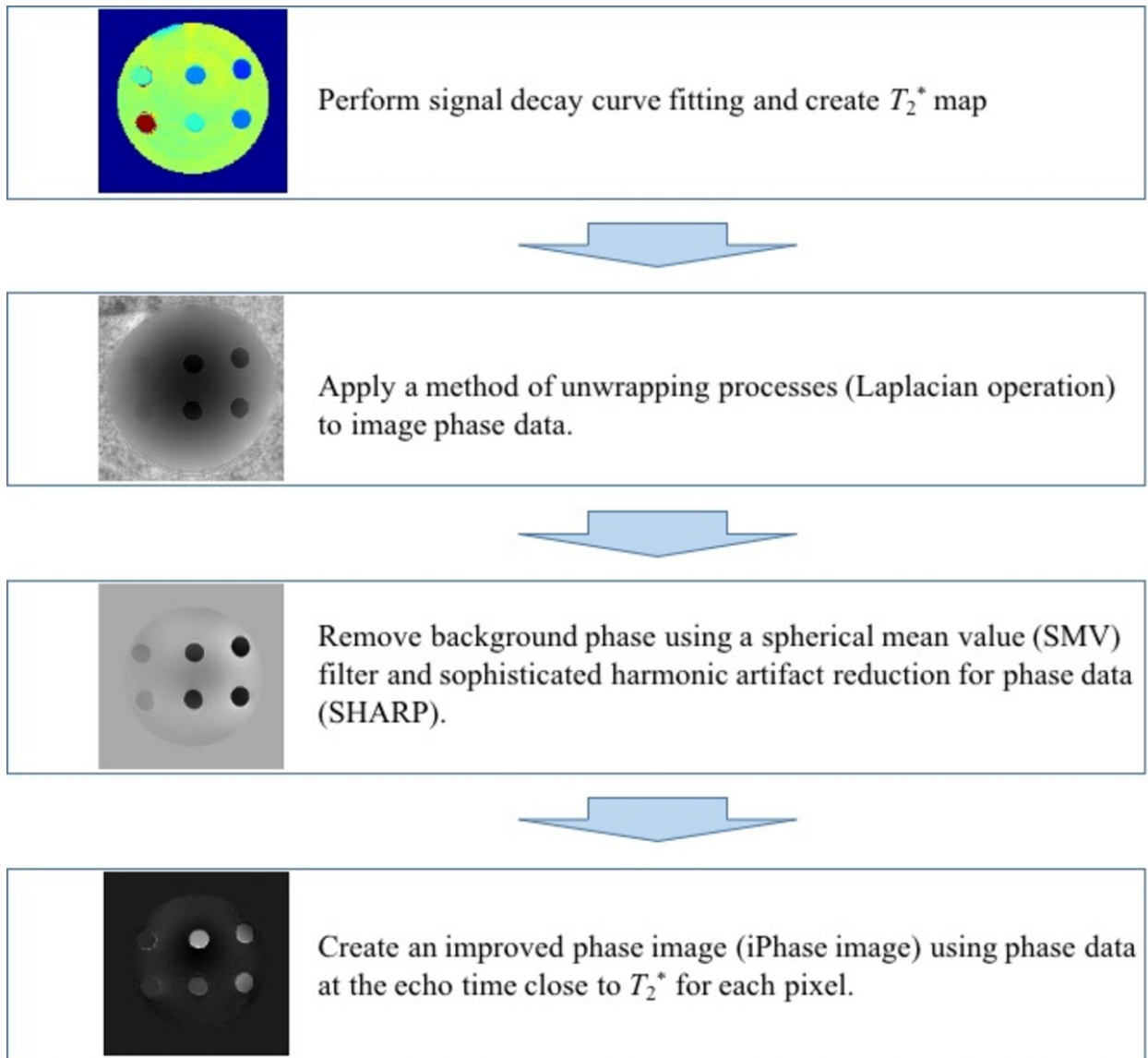


**Fig. 9:** Chart of this experiments

**References:** Tokushima University - Tokushima/JP

### 3. Data analysis

We determined regions of interest (ROIs) for each sample and calculated mean  $T_2^*$  and SD. SNRs were performed normalization at maximum phase SNR on each TE. We determined TE at maximum phase SNR and  $T_2^*$ . Coefficient of determination was calculated to confirm accuracy of  $T_2^*$  curve fitting. We applied iPhase image to SWI and calculated SNR defining using the following equation (5) :



$$SNR_{SWI} = \frac{Mean_S}{\sigma_S} \quad (5)$$

**Fig. 10**

**References:** Tokushima University - Tokushima/JP

All statistical analysis was performed using MATLAB (MathWorks, Inc., Natick, MA, USA). SMV and SHARP algorithms were used with our custom-written codes at <http://weill.cornell.edu/mri/pages/qsm.html>. We performed our analysis on a MacBook Pro (4 cores, Corei7 2.4 GHz with 16 GB RAM).

**Images for this section:**

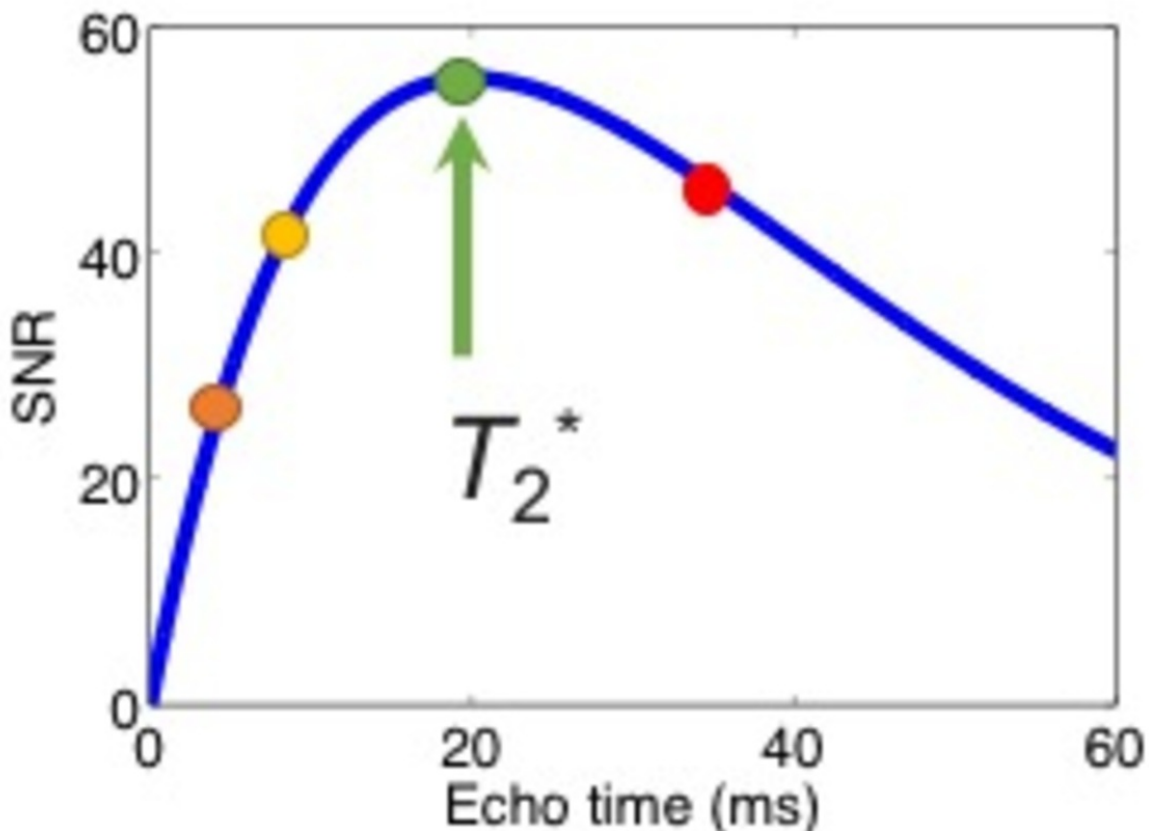


**Fig. 6:** Relationship between TE and phase SNR

© Tokushima University - Tokushima/JP

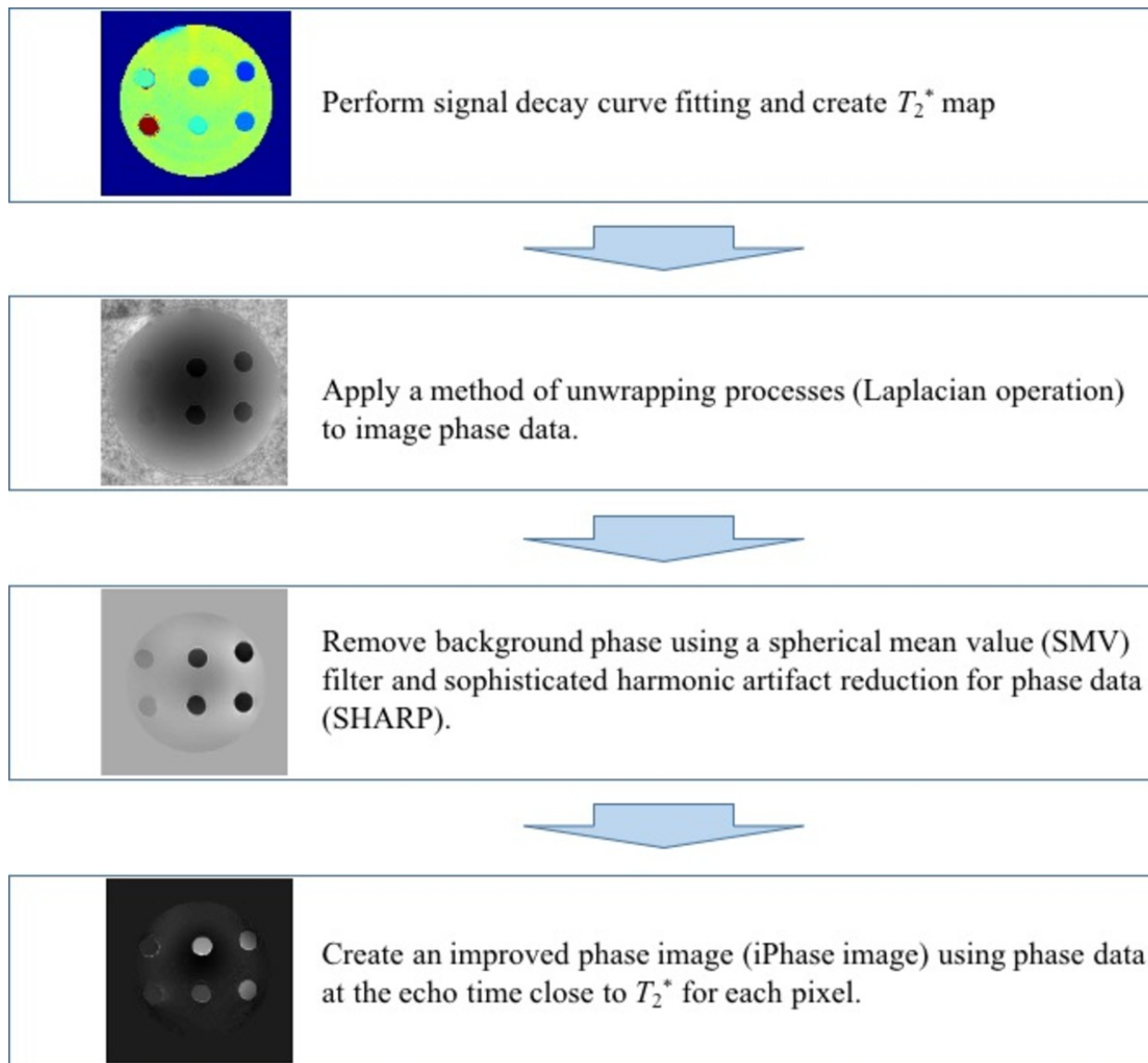


**Fig. 9:** Chart of this experiments

© Tokushima University - Tokushima/JP

## Results

Figure 11 shows measured  $T_2^*$  values for each sample of the phantom. The  $T_2^*$  fluctuation calculation was only high for the Gd-DTPA 0.1% sample when compared to the other samples.

$T_2^*$ value of each sample [ms]						
Samples	Agar+Gd 1%	Agar+Gd 0.5%	Agar+Gd 0.1%	Gd 1%	Gd 0.5%	Gd 0.1%
$T_2^*$ value	$33 \pm 0.4$	$50 \pm 0.5$	$91 \pm 2.5$	$47 \pm 0.7$	$83 \pm 1.3$	$337 \pm 92$

**Fig. 11:**  $T_2^*$  values at each sample of a phantom

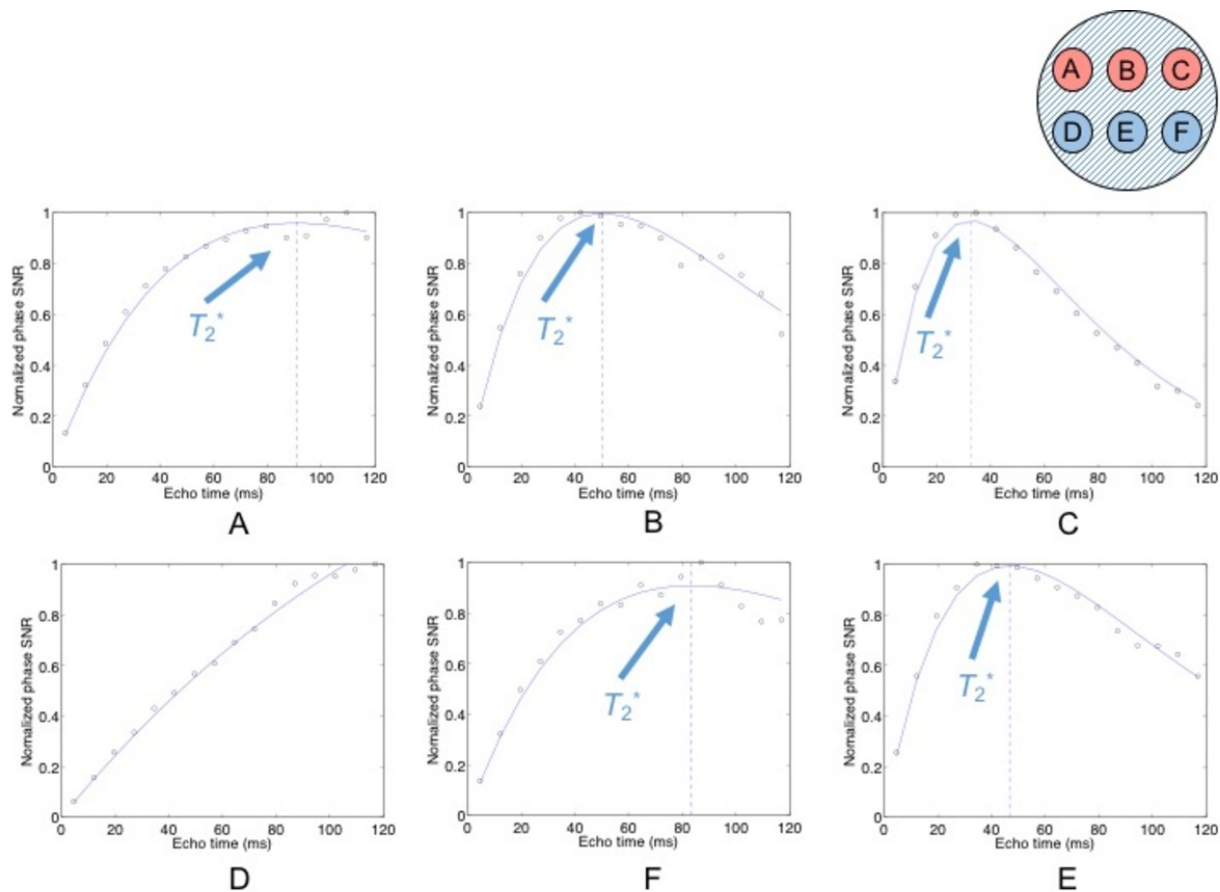
**References:** Tokushima University - Tokushima/JP

Figure 12 shows SNR values for each sample of the phantom. SWIs were derived from the conventional method and our method. SWI derived from iPhase showed in higher SNR than conventional SWI.

samples	SNR of SWI (conventional method)	SNR of SWI (iPhase meyhod)
Agar + Gd 1.0%	27.3	14.7
Agar + Gd 0.5%	17.4	24.3
Agar + Gd 0.1%	20.0	28.5
Gd 1.0%	7.4	21.7
Gd 0.5%	15.7	33.7
Gd 0.1%	19.8	29.5

**Fig. 12:** Comparison of SWIs derived from the conventional method and our method

**References:** Tokushima University - Tokushima/JP



**Fig. 13:** Relationship between TE and normalized phase SNR

**References:** Tokushima University - Tokushima/JP

Figure 13 shows the relationship between TE and normalized phase SNR in the phantom experiment. It is shown that the TE at maximum phase SNR values are close to the  $T_2^*$  of each sample.  $T_2^*$  values of each sample indicate closely at the peak of the curve between TE and phase SNR values.

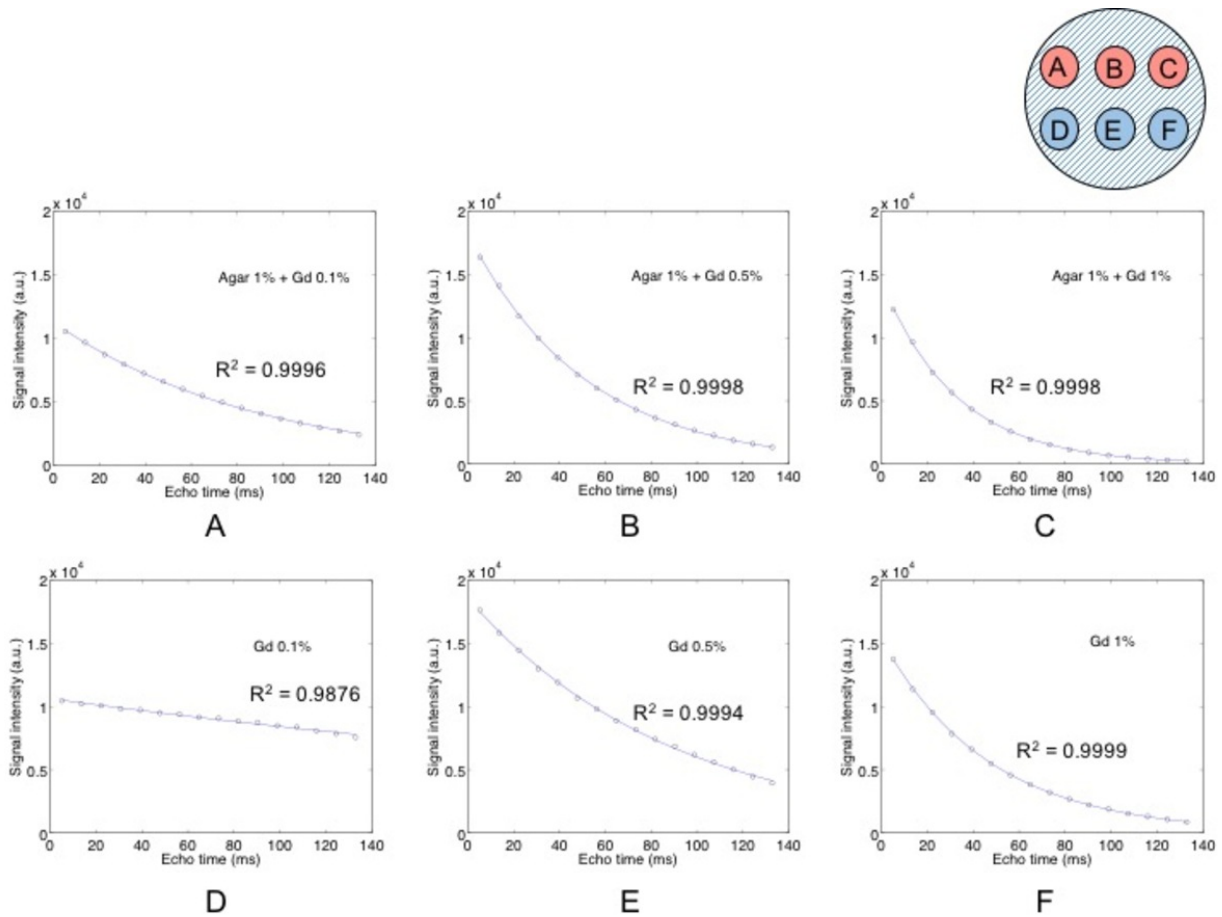


**Fig. 14:** Relationship between TE and SI

**References:** Tokushima University - Tokushima/JP

Figure 14 shows the relationship between TE and signal intensity (SI). Each plot SI and TE indicate a good fit with the data. With increase in echo number, SNR of iPhase showed a high value and good  $T_2^*$  curve fit. Our method requires accurate  $T_2^*$  curve fitting to use the  $T_2^*$  map. Then, we measured coefficient of determination. The coefficient of determination was high in value and  $T_2^*$  curve fitting was highly accurate.

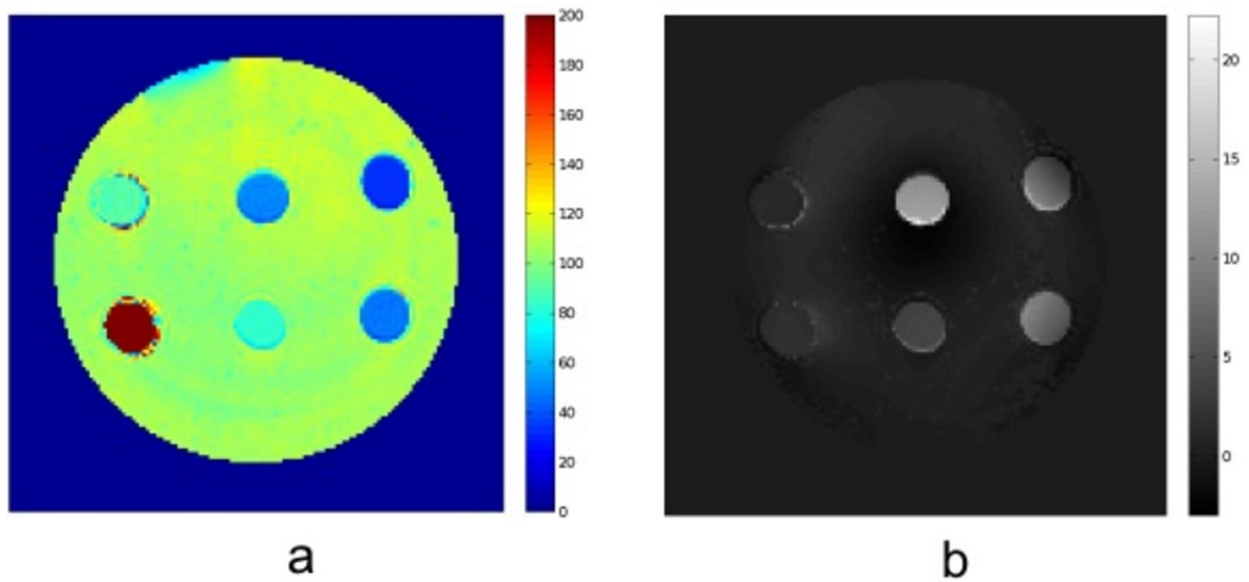


**Fig. 15:** T<sub>2</sub>\* map and iPhase image

**References:** Tokushima University - Tokushima/JP

Figure 15 shows each image derived from multi-echo 3D-SPGR of the phantom. Left, shows the  $T_2^*$  map (Fig.15a). Right, shows the iPhase image using phase data at optimized TE at each pixel (Fig.15b).

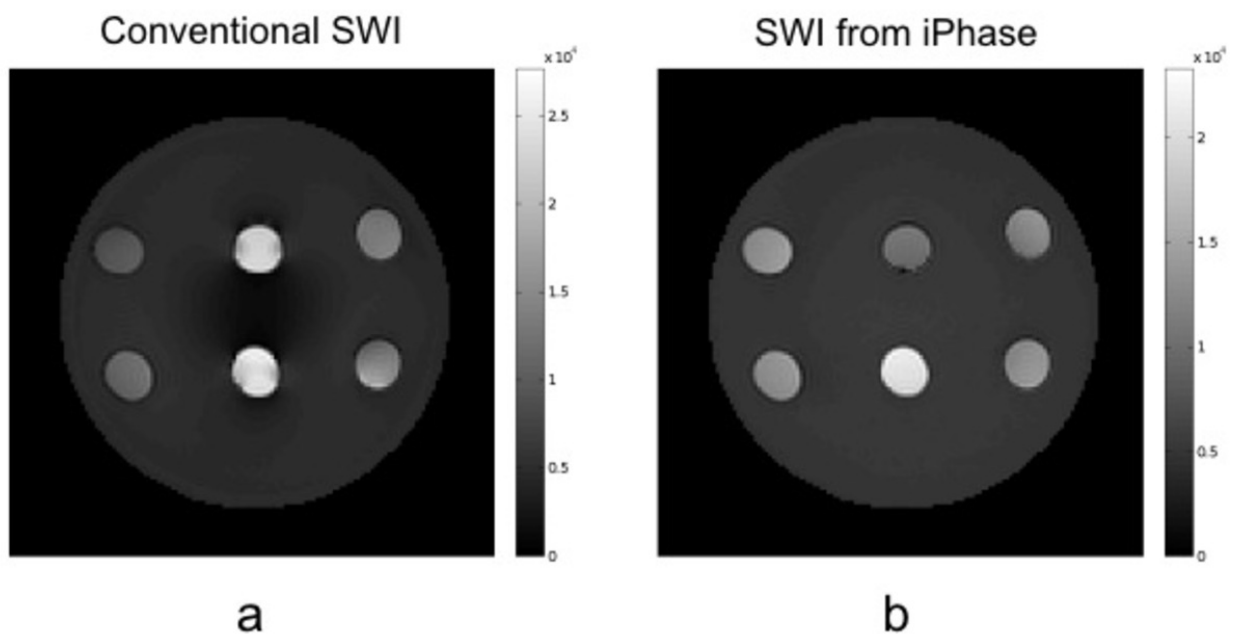


**Fig. 16:** Conventional SWI and iPhase method SWI

Figure 16 shows a comparison of two phantom images. The conventional SWI (Fig.16a), and the SWI derived from iPhase image in our method (Fig.16b). The conventional SWI is only able to emphasize the susceptibility in each pixel [3]; it is reconstructed after the phase images are high-pass-filtered and transformed to a phase mask that varies in amplitude between zero and one. This method differs vastly from our method in a great deal in physical concept of  $T_2^*$  decay. Here, to evaluate the improvement of phase SNR, we compared the SNR of SWI applied iPhase method and conventional SWI in a phantom experiment. The results showed that five of the six samples significantly were improved in each SNR, and one sample (at agar + Gd-DTPA 1.0%) was had a low-SNR (Fig. 12 and Fig 16).

Images for this section:

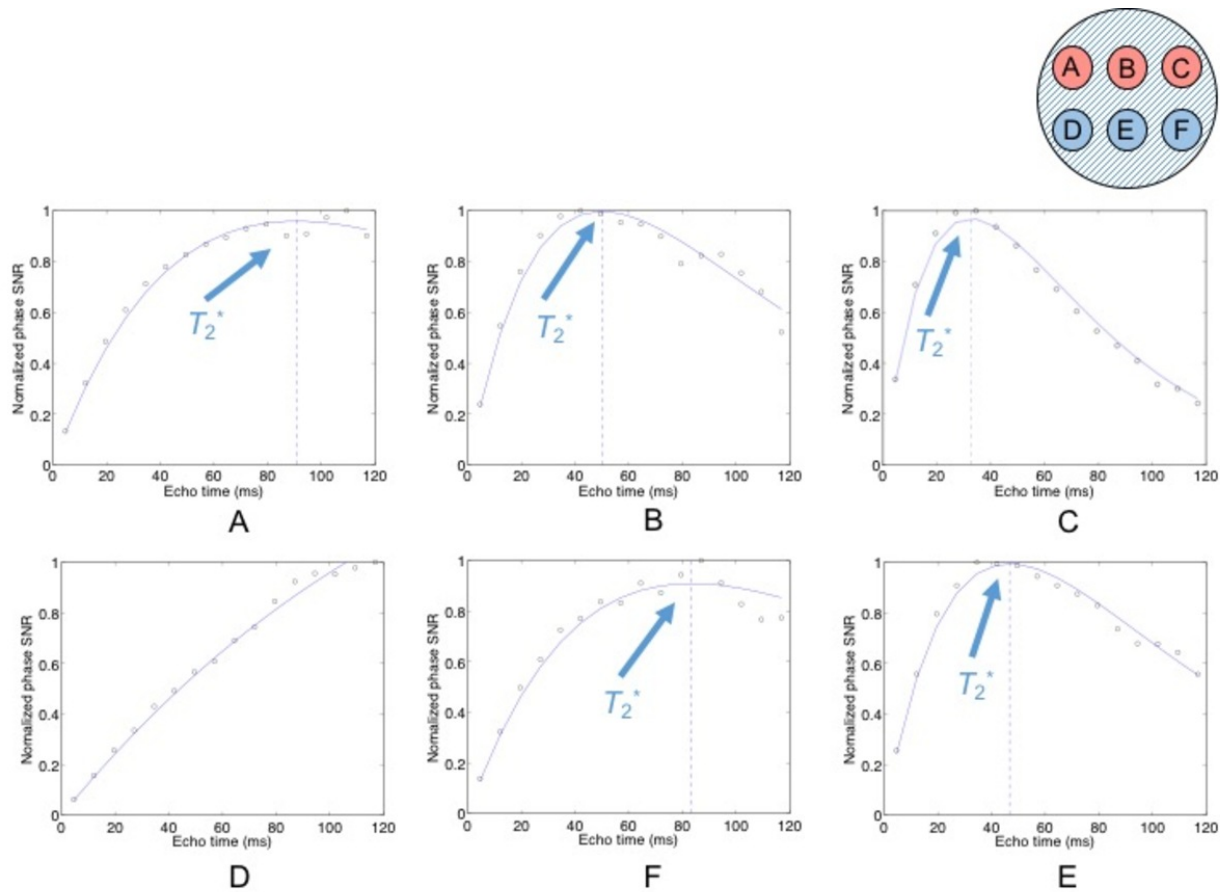
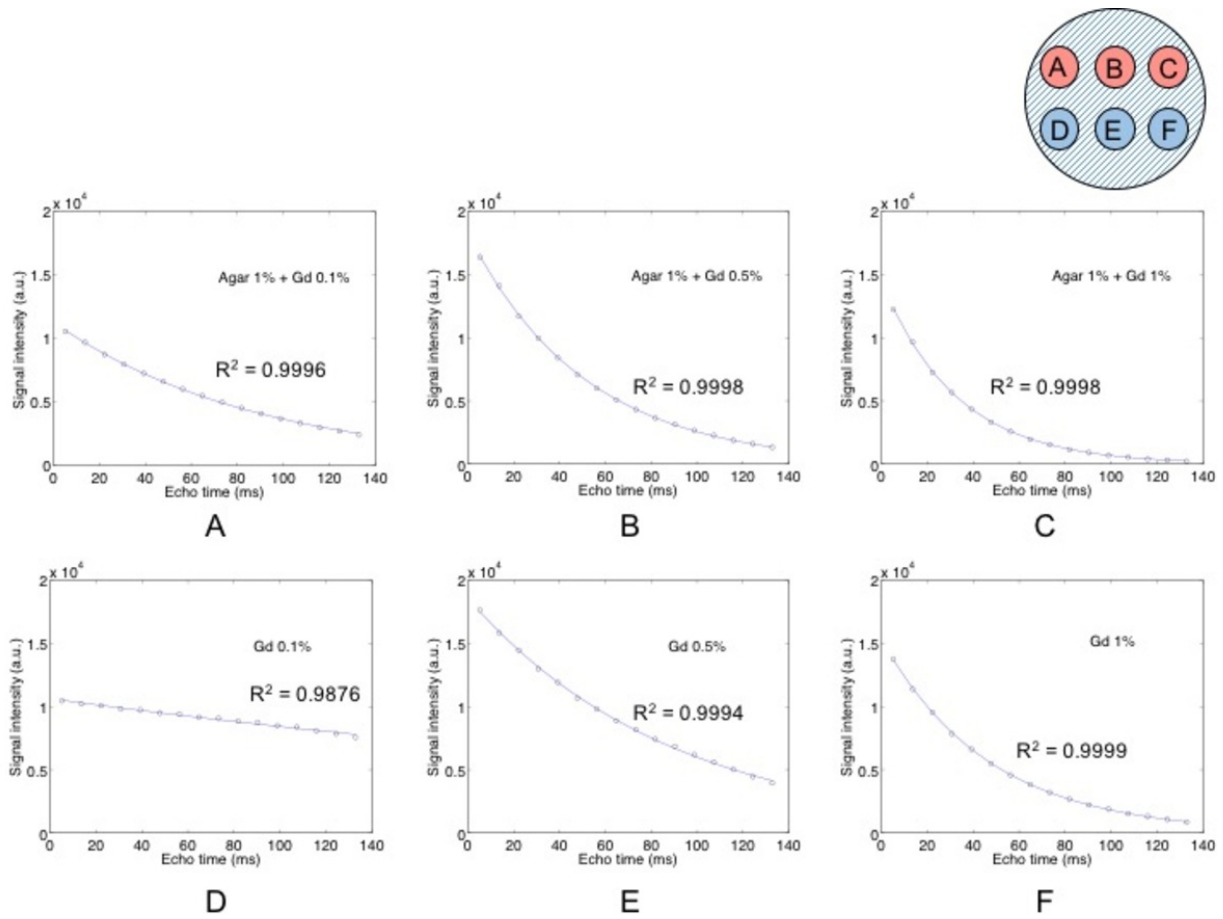


Fig. 13: Relationship between TE and normalized phase SNR

© Tokushima University - Tokushima/JP





**Fig. 14:** Relationship between TE and SI

© Tokushima University - Tokushima/JP

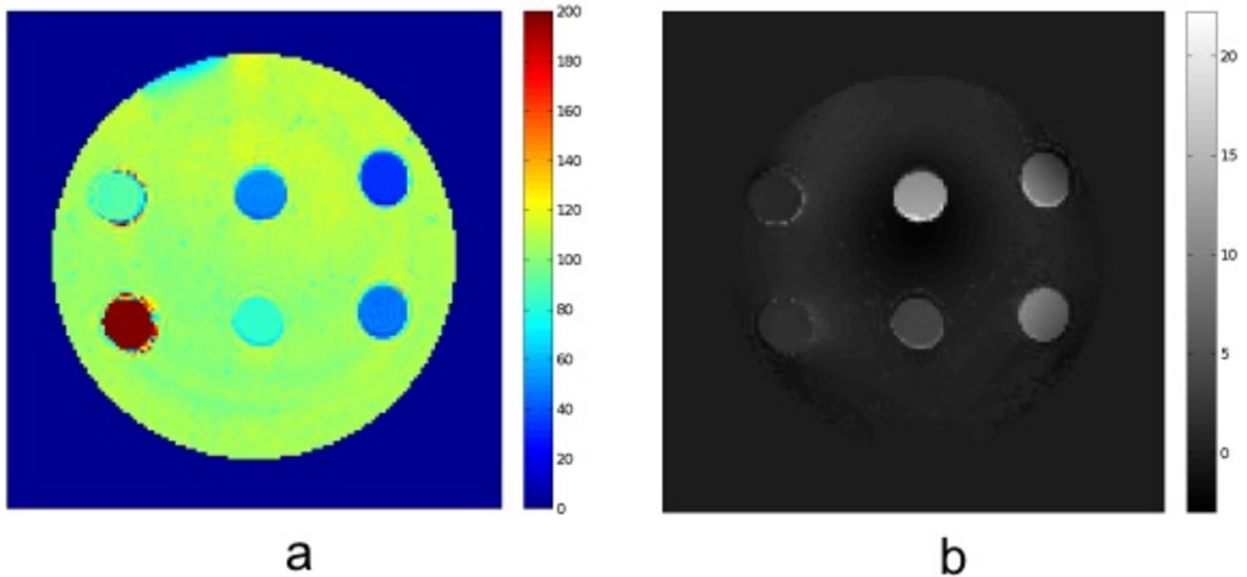




**Fig. 15:** T2\* map and iPhase image

© Tokushima University - Tokushima/JP

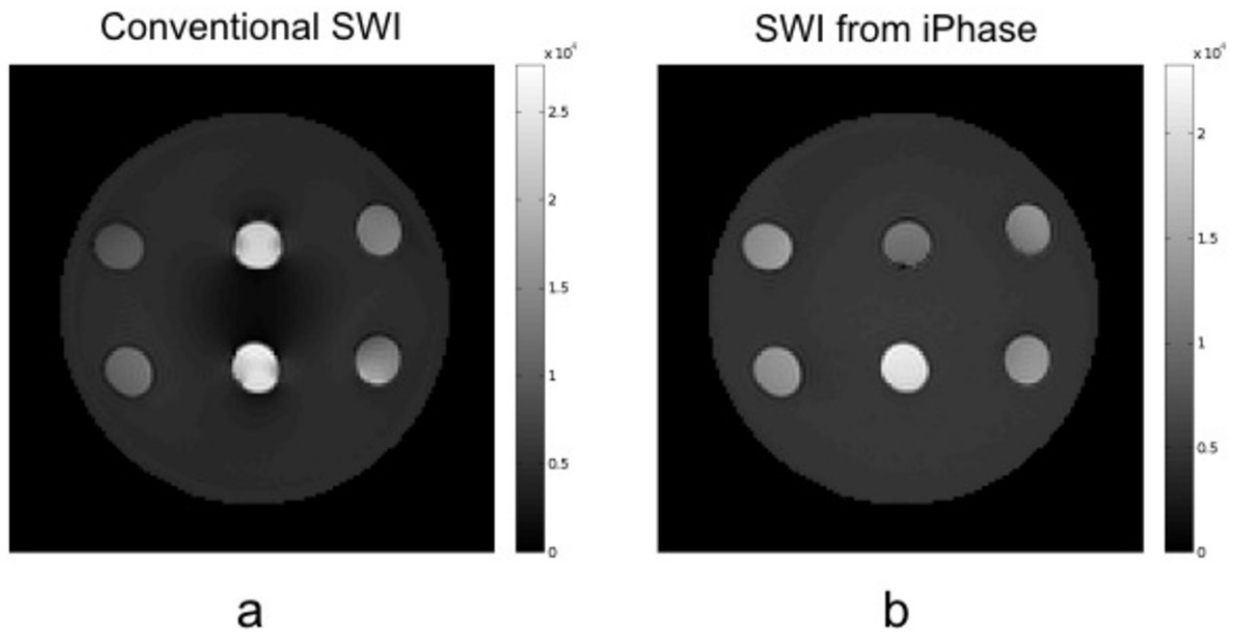


**Fig. 16:** Conventional SWI and iPhase method SWI

© Tokushima University - Tokushima/JP

## Conclusion

We developed the iPhase image method for correction for SNR using a  $T_2^*$  phase cycle of multi-echo SPGR data. The iPhase image was able to improve the image phase SNR. Moreover, our method makes it possible to obtain a phase image at a good SNR for an image affected by susceptibility, e.g., susceptibility weighted image (SWI).

## Personal information

Author Names:

Natsuki Ikemitsu<sup>1</sup>, Yuki Kanazawa<sup>2</sup>, Yuki Matsumoto<sup>1</sup>, Hiroaki Hayashi<sup>2</sup>, Takatoshi Usuda<sup>1</sup>, Toshiaki Sasaki<sup>1</sup>, Mitsuharu Miyoshi<sup>3</sup>, and Masahumi Harada<sup>2</sup>

Author Affiliations:

<sup>1</sup>School of Health Sciences, Tokushima University

<sup>2</sup>Institute of Biomedical Sciences, Tokushima University Graduate School

<sup>3</sup>MR Applications and Workflow Asia Pacific GE Healthcare Japan Corporation

Corresponding Author and Reprint Info:

Yuki Kanazawa, PhD

Institute of Biomedical Sciences, Tokushima University Graduate School 3-18-15, Kuramoto-Cho, Tokushima City, Tokushima, 770-8509, Japan E-mail: yk@tokushima-u.ac.jp

## References

1. Bock J, Kreher BW, Hennig J, and Markl M. Optimized pre-processing of time-resolved 2D and 3D Phase Contrast MRI data. Proc. Intl. Soc. Mag. Reson. Med. 15 (2007).
2. Sood S, Urriola J, Reutens D, O'Brien K, Bollmann S, Barth M, Vegh V. Echo Time-Dependent Quantitative Susceptibility Mapping Contains Information on Tissue properties. Magn Reson Med. 2016 May 25.

3. Haacke EM, Xu Y, Cheng YC, Reichenbach JR. Susceptibility Weighted Imaging (SWI). *Magnetic Resonance in Medicine* 52:612-618 (2004).
4. Wu B, Li W, Avram AV, Gho SM, Liu C. Fast and tissue-optimized mapping of magnetic susceptibility and T2\* with multi-echo and multi-shot spirals. *Neuroimage*. 2012 Jan 2;59(1):297-305.